| 1 | The Effect of Filter Storage Conditions on |
|----|--|
| 2 | Degradation of Organic Aerosols |
| 3 | Chase K. Glenn ^a , Omar El Hajj ^a , Rawad Saleh ^{a*} |
| 4 | |
| 5 | ^a Air Quality and Climate Research Laboratory, School of Environmental, Civil, Agricultural and |
| 6 | Mechanical Engineering, University of Georgia, Athens, GA, USA |
| 7 | |
| 8 | |
| 9 | *To whom correspondence should be addressed. rawad@uga.edu (706) 542-6110 |
| 10 | |

Abstract:

Current practices involve wrapping organic aerosol (OA) filter samples with aluminum foil and storing in a freezer to avoid sample degradation prior to analysis. However, there is a lack of evidence supporting these practices. Here, we investigate the effect of thermal and photo degradation on toluene-combustion OA, pine-combustion OA, and ambient OA samples by storing them in petri dishes for one month at three different conditions: covered with aluminum foil and in a freezer (F), covered with aluminum foil at room temperature (RC), and uncovered at room temperature (RUC). We performed three types of analyses: thermal-optical measurements, electrospray ionization mass spectrometry, and UV-vis spectroscopy. For all samples, we observed a mild reduction in the relatively volatile organic carbon fraction (OC1) in the RC and RUC conditions. We did not account for positive artifacts in this study, and therefore, this reduction was at least partially due to evaporation of adsorbed vapors rather than particles. There was no evidence of significant systematic change in chemical composition relative to control for any of the storage conditions, except for loss of some small-molecular-size compounds in conditions RC and RUC for pine-combustion OA, likely due to evaporation. There was no evidence that photobleaching occurred in the RUC condition for any of the samples. On the contrary, we observed an increase in absorption in the RC and RUC conditions for pine-combustion OA, likely due to evaporation of small-molecular-size species with relatively weak absorption.

1. Introduction

Aerosols are often collected on filters for offline analyses days or weeks after sample collection. One of the most common of these analyses is quantifying the elemental carbon (EC) and organic carbon (OC) fractions of aerosol particles collected on Quartz filters via thermaloptical techniques (Chow et al., 2007, 2011, 2015; Kuwayama et al., 2015; Massabò et al., 2016; Perrino et al., 2019). For example, filters are collected routinely for OCEC analysis at EPA's 51 Chemical Speciation Network (CSN) and 110 Interagency Monitoring PROtected Visual Environments (IMPROVE) sites all around the U.S. (EPA, 2009). There is a wealth of other offline chemical speciation methods that rely on filter collection, the majority of which focus on speciating the organic molecules in the aerosol, to various degrees of detail, using chromatography and mass spectrometry techniques (Johnston & Kerecman, 2019; Qi et al., 2022). Another ubiquitously employed technique is UV-vis spectroscopy, which can be used to retrieve the wavelength-dependent light-absorption properties of light-absorbing organic aerosol, or brown carbon (BrC) (Atwi, Cheng, et al., 2022; Z. Cheng et al., 2021; Islam et al., 2022).

A common practice, often mentioned in the methods sections of papers that involve offline analyses of aerosol filter samples, is to cover the filters (e.g. in aluminum foil) and store them in a freezer. Though usually not explicitly stated, the reason for these filter-storage practices is presumably to prevent thermal degradation and/or photo-degradation of the aerosol sample between collection and analysis. Here, the terms thermal degradation and photo-degradation are used broadly to indicate changes in the aerosol sample composition driven by, respectively, temperature and exposure to light. Thermal decomposition of organic aerosol (OA) molecules is well-documented and has been shown to occur in chemical-speciation instruments that rely on thermal desorption to vaporize the OA molecules for ionization (Riva et al., 2019; Yang et al., 2021). Photolysis of OA molecules is also well-documented and has been extensively studied in the laboratory. Photolysis has been shown to induce both fragmentation (Bateman et al., 2011; Romonosky et al., 2017) and oligomerization (Walhout et al., 2019), as well as loss of carbonyl groups (Bateman et al., 2011; Walhout et al., 2019) in secondary organic aerosol (SOA).

Furthermore, photobleaching (destruction of chromophores by photolysis) has been shown to substantially reduce BrC absorption in the UV-visible spectrum (Browne et al., 2019; Wong et al., 2017).

It is plausible that temperature- and photo-induced chemical transformations can take place within an OA filter sample stored for long periods of time at ambient or laboratory conditions, which would justify storage in a freezer and packaging in dry ice if the sample is transported. However, evidence in the literature to support this practice is lacking. We found only one peer-reviewed study that assessed the effect of filter-storage conditions on OCEC analysis (Dillner et al., 2009). That study reported a 16% decrease in OC1 (the highest-volatility bin of the four OC bins in standard OCEC thermal-optical analysis) for filters stored for 48 hours at room temperature compared to those stored in a freezer at -16 °C. This finding was attributed to the evaporation of the relatively high-volatility organic molecules at room temperature.

In this study, we performed a systematic investigation of the effect of filter-storage conditions on OA chemical composition and light-absorption properties. We considered three OA systems that provide diversity in chemical composition and light-absorption properties: OA produced from toluene-combustion, OA produced from biomass burning, and ambient OA. We employed three filter-storage conditions to assess temperature- and photo-induced chemical transformations: covered with aluminum foil and in a freezer at -15 °C, covered with aluminum foil and at room temperature, and uncovered at room temperature. We performed three types of analyses: OCEC analysis using the thermal-optical technique, chemical speciation using electrospray ionization mass spectrometry, and light-absorption UV-vis absorption spectroscopy.

2. Methods

2.1 Aerosol sources

To assess the effect of filter-storage conditions on the analysis of aerosol physicochemical properties, we considered three organic aerosol (OA) systems obtained from the following sources: (1) controlled combustion of toluene, (2) uncontrolled combustion of dead pine needles, and (3) ambient aerosol in Athens, GA. As described below, these sources provide wide diversity in aerosol chemical composition that capture the variability in atmospheric OA.

Aromatic compounds, including toluene, constitute approximately 30% of gasoline fuel (Javed et al., 2016; Shao et al., 2019). Furthermore, toluene is often used as an additive to boost the fuel octane rating (Badia et al., 2021; Fioroni et al., 2022). We have previously shown that the aerosol emissions from toluene-combustion exhibited similar physicochemical properties to other aromatic (benzene) (Saleh et al., 2018) and aliphatic (heptane, isooctane) (Cheng et al., 2021; El Hajj et al., 2021) gasoline constituents. Therefore, in this study we employ toluene-combustion as a surrogate for on-road gasoline vehicles. Toluene-combustion was performed in a steady-flow quartz combustion chamber at a constant temperature (1000° C), equivalence ratio (1.06), and $0_2/N_2$ (0.06). This controlled combustion setup, described in detail elsewhere (Z. Cheng et al., 2019), allows for the production of a steady flow of aerosol emissions with consistent emission rates and physicochemical properties that are a function of set combustion conditions. For this study, the combustion conditions indicated above were chosen to produce aerosol dominated by organics (i.e. OA) with negligible contribution from black carbon (BC). We have previously shown that toluene-combustion OA consists mostly of polycyclic aromatic hydrocarbons (PAHs) with varying molecular sizes (Atwi et al., 2021; El Hajj et al., 2021; Saleh et al., 2018). These

PAHs are non-polar and belong to the family of light-absorbing organic aerosol, or brown carbon (BrC).

Dead pine needles constitute a ubiquitous component of surface fuels in wildlands in the U.S. and are usually consumed in prescribed fires and wildfires (Stubbs et al., 2021; Susaeta & Gong, 2019). We burned the pine needles inside a 7.5 m³ environmental chamber in a procedure similar to (Atwi, Cheng, et al., 2022; Atwi, Wilson, et al., 2022). The relative abundance of OA and BC in the emissions of biomass combustion depends largely on combustion conditions (flaming versus smoldering) (L.-W. A. Chen et al., 2007; Lee et al., 2005a; McMeeking et al., 2009; Reid et al., 2005). In this study, the combustion was smoldering, and the aerosol emissions were predominantly organic. Because of the complexity of the chemical composition of biomass fuels, the OA emissions also exhibit complex chemical composition. OA species observed in biomass-burning emissions include oxygenated and nitrated molecules such as nitro-aromatics, organic nitrogen species, among others (Bhattarai et al., 2019; Laskin et al., 2009; Lee et al., 2005b; Lin et al., 2016; H. Zhang et al., 2018). Therefore, the combustion of pine needles provides an aerosol system with higher polarity and substantially more molecular diversity compared to toluene.

Ambient aerosol was collected from the 3rd floor of the Interdisciplinary STEM building on the campus of the University of Georgia (UGA) during the month of May 2022. The sampling location is in the vicinity of regions that feature urban activity as well as high levels of vegetation cover. Therefore, the ambient aerosol is expected to include a combination of relatively fresh anthropogenic primary organic aerosol (POA), as well as secondary organic aerosol (SOA) from both anthropogenic and biogenic sources. Both field measurements (Heald et al., 2020; H. Zhang et al., 2018) and modeling studies (Goldstein et al., 2009; Neyestani et al., 2020) have shown that background OA in the Southeastern U.S. is dominated by biogenic SOA during the summer months, thus biogenic SOA is expected to be ubiquitous in the ambient samples in this study.

2.2 Sample collection, preparation, and storage conditions

The aerosols from each source were collected on one 47 mm Quartz filter (PALL, Tissuquartz 2500) and one 47 mm polytetrafluoroethylene (PTFE) filter (0.2 microns, Sterlitech Corporation). We targeted an aerosol loading of approximately 300 μg on each filter from the combustion of toluene and pine needles. The required sampling time was estimated from the flow rate through each filter (5 LPM) and total aerosol mass concentration obtained from integrating continuous size distribution measurements using a scanning mobility particle sizer (SMPS, TSI 3882). As shown in SI Figure S1, the aerosol mass concentration was steady at approximately 250 $\mu g/m^3$ during the course of the toluene-combustion experiment. On the other hand, the concentration of aerosol emissions from the combustion of pine needles dropped from approximately 460 $\mu g/m^3$ to 170 $\mu g/m^3$ during the course of the experiments due to wall losses in the environmental chamber. Ambient aerosol samples were collected at a flow rate of 5 LPM through each filter over the course of 72 hours. This collection occurred over the weekend through Monday, encompassing both high and low anthropogenic activities.

After collection, the quartz filters were divided into four 1.5 cm² rectangular punches and the PTFE filters were divided into four quadrants. One quartz punch and PTFE quadrant were analyzed immediately (control) as described below. The others were stored for one month in a sterilized petri dish (PALL, AnalyslideTM) prior to analysis at three different storage conditions: (i) covered with aluminum foil and in the freezer at -15°C (hereafter referred to as condition 'F'),

(ii) at room temperature and covered with aluminum foil (hereafter referred to as condition 'RC'), and (iii) at room temperature and uncovered (hereafter referred to as condition 'RUC').

The quartz punches were used directly for OCEC analysis as described in Section 2.3. The PTFE filter quadrants were first extracted in an organic solvent, and the extracts were used for chemical speciation (Section 2.3) and UV-vis absorption measurements (Section 2.4). Methanol (Sigma-Aldrich, HPLC ≥ 99.9%) was used as a solvent for pine-needle combustion OA and ambient OA. We chose methanol because of its efficacy at extracting organic species with a wide variation of polarity, and due to its use in previous studies with both biomass-burning aerosol (Atwi, Cheng, et al., 2022; Y. Chen & Bond, 2010) and ambient aerosol (Y. Cheng et al., 2016; Verma et al., 2012). We used dichloromethane (DCM) (Sigma-Aldrich, HPLC ≥ 99.9%) to extract toluene-combustion OA because of its efficacy at extracting non-polar organic species, including PAHs (Apicella et al., 2007; Z. Cheng et al., 2021; Michela et al., 2008; Russo et al., 2013).

The extraction procedure involved immersing the PTFE filter quadrants in 3.5 ml of solvent and sonicating for 10 minutes. Insoluble species that were mechanically dislodged from the filters during sonication were filtered from each solution using a glass lure lock syringe with a 13mm PTFE filter (0.2 microns, Sterlitech Corporation). Blanks were prepared by extracting clean PTFE filter quadrants in methanol and DCM following the same process.

2.3. Chemical speciation

The quartz filter punches were analyzed in an OCEC Analyzer (Sunset Laboratory, Model 5 L) following the NIOSH-870 protocol (Wu et al., 2016) (see SI Table S1). The NIOSH-870 protocol distributes the OC into four bins (OC1, OC2, OC3, OC4) that are operationally defined based on the stepwise increase in oven temperature during the analysis. Furthermore, part of the OC gets pyrolyzed (charred) during the OC analysis phase and is oxidized and detected as EC during the EC analysis phase. A correction algorithm is employed to retrieve the pyrolyzed OC (PyroOC) fraction (Chow et al., 2007) which is reported in a separate bin.

The methanol-soluble pine-needle combustion OA and ambient OA samples were analyzed using ultra-high-resolution electrospray ionization mass spectrometry (ESI-MS). ESI-MS has been used extensively to analyze the chemical composition of OA in biomass combustion emissions (Atwi, Wilson, et al., 2022; Ijaz et al., 2022; Laskin et al., 2009; Lin et al., 2017, 2018; Schneider et al., 2022; Smith et al., 2009) and ambient aerosol (X. Zhang et al., 2013) because these aerosol systems include molecules with ionizable functional groups that are responsive to ESI (Laskin et al., 2015; Nizkorodov et al., 2011). ESI-MS analysis was performed on a Bruker SolariX XR 12T Fourier-transform ion cyclotron resonance (FTICR) mass spectrometer in negative ionization mode over m/z range of 74 – 600. Samples were ionized at a source rate of 2 uL/min with the capillary set to 4500 V and an end plate offset of -800 V. The nebulizer gas pressure was 0.8 bar, dry gas rate was 4.0 L/min, and the dry temp was 200 C. The resulting mass spectra were analyzed using the open-source software MFassignR (Schum et al., 2020). Sample noise was calculated using the built-in KMDNoise function and the data was filtered to include only peaks with S/N threshold ≥ 3 . After an initial C, H, O assignment, C^{13} and S^{34} isotopes were identified and filtered. Following a built-in mass recalibration, the final formula assignments were obtained using elemental constraints of $N \le 3$ and $S \le 1$. The methanol blank was analyzed using the same settings and the resulting background peaks were removed from the sample mass spectra. We did not perform ESI-MS analysis on toluene-combustion OA because it is predominantly composed of PAHs (El Hajj et al., 2021; Saleh et al., 2018), which are not efficiently detected with ESI (Bateman et al., 2011).

2.4. Light-absorption properties

The absorbance of the OA solutions was measured using a UV-vis spectrometer (Agilent, Cary 60) between 400 - 600 nm at a 1 nm resolution. The presence of BrC manifests as a power-law increase in absorption with decreasing wavelength. The absorption spectra of BrC can exhibit some features if the BrC has relatively uniform molecular structure (e.g. in the combustion emissions of single-molecule fuels (Z. Cheng et al., 2021), but is often featureless for BrC with diverse molecular structures (e.g. in biomass-burning emissions (Islam et al., 2022)). While the different BrC chromophores contribute differently to absorption at each wavelength, one can define mean bulk BrC light-absorption properties. We retrieved the mean BrC imaginary part of the refractive index (k) for the wavelength range 400 nm - 600 nm following the procedure of (Atwi, Cheng, et al., 2022; Z. Cheng et al., 2021). To do so, we calculated the absorption coefficient as:

$$\alpha = \frac{\ln(10) \,\mathrm{A} \,\rho}{\mathrm{C}_{\mathrm{BrC}} \,\mathrm{L}} \tag{1}$$

Where α (cm⁻¹) is the absorption coefficient, A is the absorbance, ρ is the BrC density (assumed to be 1.2 g cm⁻³), L (1 cm) is the optical path length, and C_{BrC} (g cm⁻³) is the BrC concentration in the solution. To estimate C_{BrC} , we deposited 250 μ l of each solution on a pre-baked quartz filter punch, allowed the solvent to evaporate under a steam of clean air, and quantified the carbon content (OC) using the OCEC analyzer following the same procedure described in Section 2.3. We then converted the retrieved α to k values as:

$$k = \frac{\lambda \, \alpha}{4 \, \pi} \tag{2}$$

3. Results and discussion

3.1. Physicochemical properties of the three organic aerosol systems

As described in Section 2.1, the sources employed in this study (toluene-combustion, pine-combustion, and ambient) were chosen to yield OA systems with diverse physicochemical properties. In this section, we compare the chemical composition and light-absorption properties of the control samples (i.e., analyzed immediately after collection) of the three OA systems.

Figure 1 shows the break-down of the OC fractions. Toluene-combustion OA has the highest volatility, followed by pine-combustion OA and ambient OA, as signified by the relative abundance of the OC1-4 fractions. PyroOC is most abundantly represented in ambient OA, followed by pine-combustion OA and toluene-combustion OA. This suggests that the lower volatility, more oxidized OA chars more efficiently in the initial oxygen-deficient phase of the analysis.

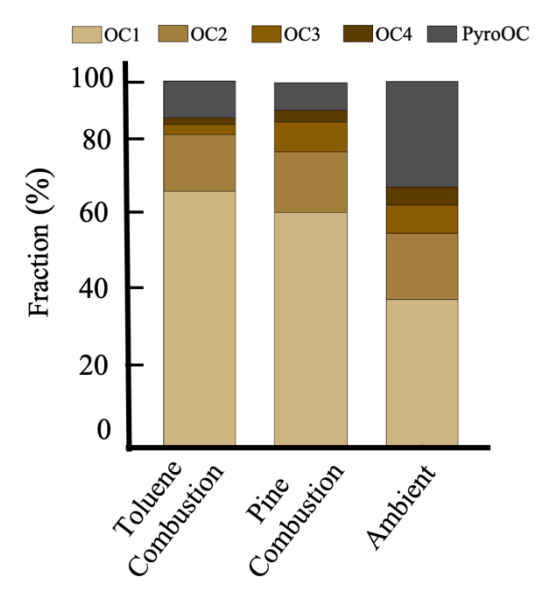


Figure 1. Fractions of the different OC bins for the control samples of toluene-combustion OA, pine-combustion OA, and ambient OA.

The mass spectra of the pine-combustion OA and ambient OA obtained using ESI-FTICR-MS are shown in Figure 2a and 2b, respectively. The pine-combustion OA mass spectrum includes peaks with molecular formulas that likely correspond to molecules associated with biomass-burning OA. A few examples are indicated on Figure 2a, such as levoglucosan ($C_6H_{10}O_5$) (Bhattarai et al., 2019), Retene ($C_{18}H_{18}$) (Simoneit, 2002), and $C_7H_6N_2O_6$ (Wang et al., 2019). The ambient OA mass spectrum (Figure 2b) also includes a peak that likely corresponds to levoglucosan, which suggests contribution from biomass burning. Furthermore, the ambient OA mass spectrum includes peaks that are likely biogenic SOA markers, such as $C_4H_8O_4$ and $C_7H_{10}O_4$ (Mahilang et al., 2021), as well as anthropogenic SOA markers, such as $C_9H_{16}SO_7$ and $C_{16}H_{22}SO_6$ (Blair et al., 2017). The pine-combustion OA had average O:C = 0.31 and H:C = 1.48, while the ambient OA had average O:C = 0.60 and H:C = 1.4. These values indicate that the ambient OA, having undergone atmospheric aging, is more oxidized and less saturated than the pine-combustion OA.

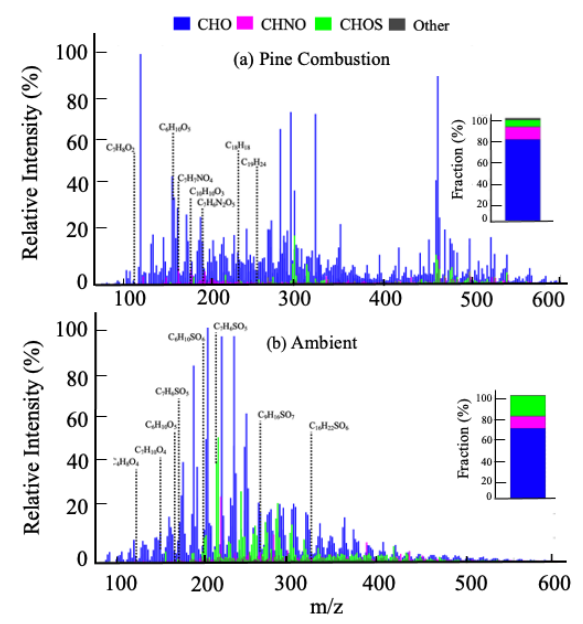


Figure 2. Mass spectra obtained using ESI-FTICR-MS for the control samples of (a) pine-combustion OA and (b) ambient OA. The inserts represent the intensity-weighted fractions of elemental groups.

As shown in Figure 2, the majority of organic molecules detected by ESI-MS were CHO in both pine-combustion OA (79%) and ambient OA (68%), followed by CHNO (12.5% for pine-combustion OA and 12% for ambient OA) and CHOS (6% for pine-combustion OA and 12% for ambient OA). The ambient CHOS species included a series of chemical formulas, which are associated with biogenic SOA (Hettiyadura et al., 2019; Kristensen & Glasius, 2011), but are also shown to be produced from the photo-oxidation of diesel and biodiesel fuels (Blair et al., 2017).

The imaginary part of the refractive indices (k) retrieved for wavelengths between 400 nm, and 600 nm are shown in Figure 3. The DCM extracts of toluene-combustion OA have k values that are an order of magnitude larger than those of the methanol extracts of pine-combustion OA, indicating that DCM extracts of toluene-combustion OA had BrC species with significantly stronger absorption. We were not able to obtain reliable UV-vis absorbance signals for the ambient OA samples due to the low concentrations of the samples and possibly their inherent weak absorption. Therefore, we were not able to retrieve k for the ambient OA samples.

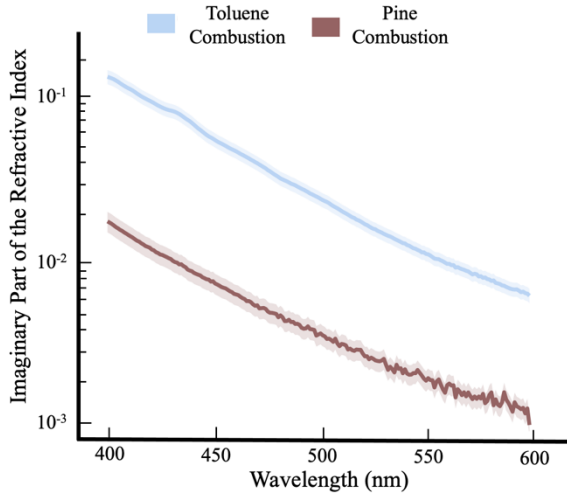


Figure 3. Imaginary part of the refractive indices (k) of OA extracts for the control samples of toluene-combustion OA and pine-combustion OA. Shaded regions depict uncertainty bounds, calculated as shown in the SI.

3.2. Effect of filter-storage conditions on thermal-optical measurements

The fractions of the different OC bins obtained from the OCEC analyzer for the different filter-storage conditions are shown in Figure 4. For toluene-combustion OA, the OC1 fraction dropped from 70% for control to 58% and 50% for conditions RC and RUC, respectively. The reduction in OC1 fraction can be attributed to the evaporation of the relatively volatile organic species in OC1 (Dillner et al., 2009). Notably, the reduction in OC1 fraction led to an increase in PyroOC fraction from 10% for control to 17% and 23% for conditions RC and RUC, respectively. This result suggests that the relatively volatile organics in OC1, which evaporated in conditions RC and RUC, were less susceptible to pyrolysis during OCEC analysis. Pine-combustion OA exhibited a similar but less prominent reduction in OC1 from 65% for control to 60% and 52% for conditions RC and RUC, respectively. Ambient OA was the least susceptible to reduction in OC1 fraction. These results suggest that the OC1 compounds in ambient OA were the least volatile, followed by pine-combustion OA and toluene-combustion OA.** Discuss on Monday**

Collection of organic aerosols on quartz filters is susceptible to positive artifacts due to adsorption of vapors (Y. Cheng et al., 2010; Turpin et al., 1994, 2000). In this study we did not correct for these artifacts. Therefore, the reduction in OC1 in conditions RC and RUC compared to control for the toluene-combustion and pine-combustion OA was at least partially due to loss of adsorbed vapors rather than particles (Dillner et al., 2009).

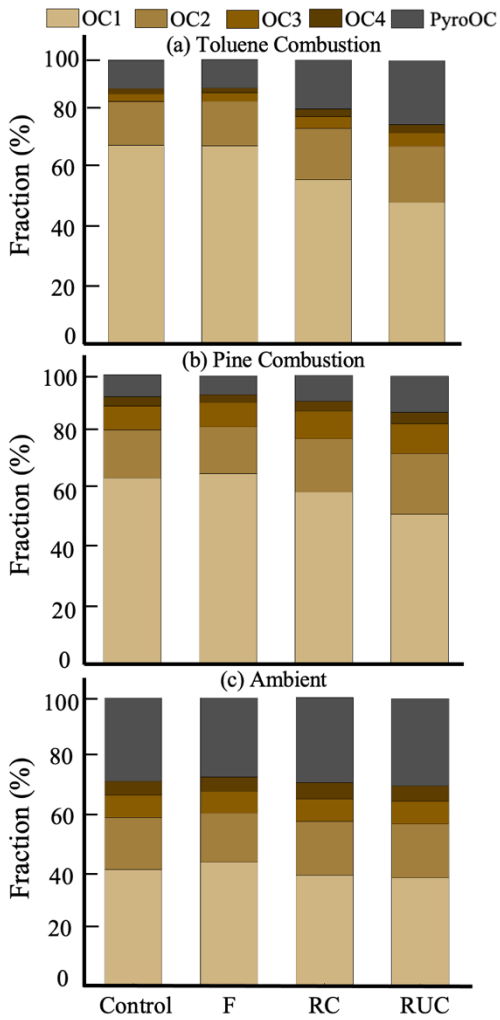


Figure 4. Fractions of the OC bins for samples stored at different conditions for (a) toluene-combustion OA, (b) pine-combustion OA, and (c) ambient OA.

3.3. Effect of filter-storage conditions on ESI-FTICR-MS measurements

To assess changes in chemical composition induced by the different storage conditions relative to control, we calculated the observed change in each species (i.e. each peak in the mass spectrum) following the approach of (Bateman et al., 2011):

$$\alpha_{i} = \frac{X_{i}^{S}}{X_{i}^{control}} \tag{3}$$

Where, X_i is the relative intensity of peak i in the mass spectrum and superscript S corresponds to the different storage conditions (F, RU, and RUC).

We grouped the species based on their α values into five categories: Increased ($\alpha > 2$), Decreased ($\alpha < 0.5$), No Change ($0.5 \le \alpha \le 2$), Obliterated ($\alpha = 0$), and New ($\alpha =$ 'infinity'). We then calculated the relative-intensity-weighted fraction of each category for the different storage conditions. The fractions of the No Change, Increased, Decreased, and Obliterated categories were calculated based on the relative intensities of the control mass spectrum. In other words, this calculation addresses the question: what fraction of species in the control spectrum underwent a certain observed change (No Change, Increased, Decreased, Obliterated) due to the different storage conditions? The fraction of the New category was calculated based on the relative

intensities of the storage condition mass spectrum. In other words, this calculation addresses the question: what fraction of the species in the mass spectrum of each storage condition corresponds to new species that did not exist in the control mass spectrum?

No Change Decreased Increased Obliterated New (a) Pine Combustion Fraction (%) (b) Ambient Fraction (%) F RCRUC

Figure 5. Fractions of observed change in ESI-FTICR-MS mass spectra relative to control due to different storage conditions for (a) pine-combustion OA and (b) ambient OA.

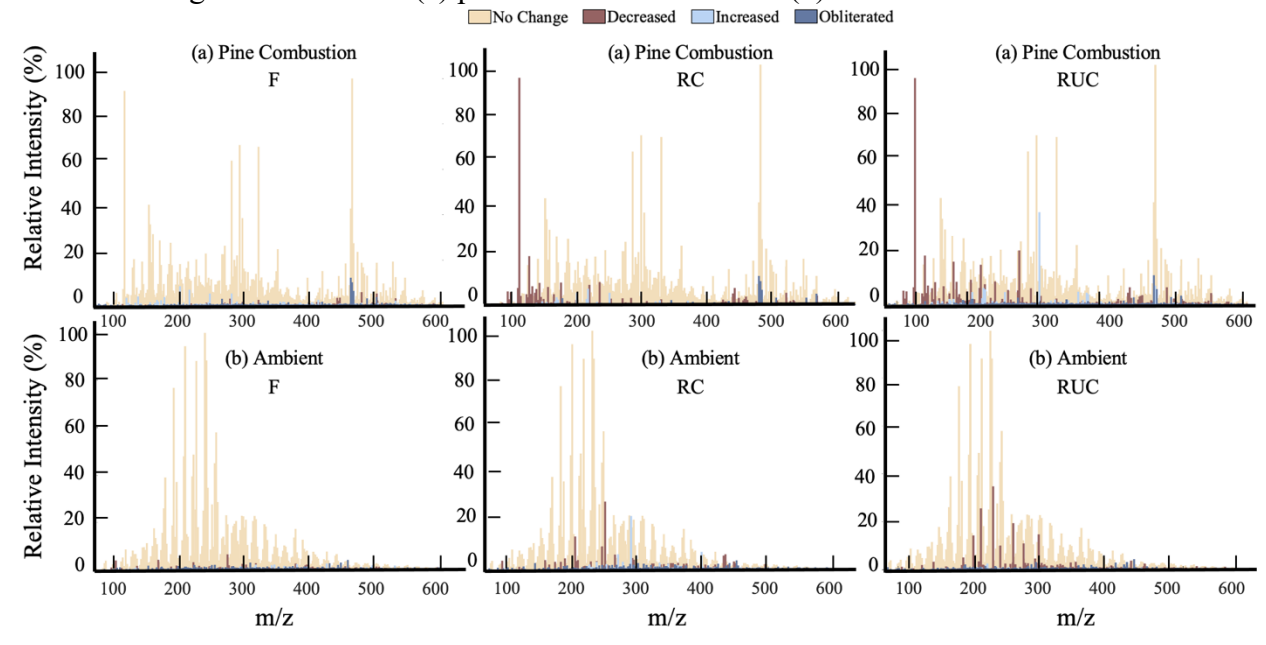


Figure 6. Mass spectra and observed changes obtained using ESI-FTICR-MS. Observed changes are storage condition samples of (a) pine combustion OA and (b) ambient OA compared to control. Color coded by observed change.

321322

323

324 325

326

327

328

329

330

331

332

333

334335

336

337338

339

340

341

342

343

344

345

346

347348

349 350

351

352

As shown in Figure 5, for both pine-combustion OA and ambient OA, the majority of the species underwent relatively small change due to storage. There are several physical and/or chemical transformation pathways that can potentially account for the observed changes (Increased, Decreased, and Obliterated). Those include evaporation of relatively volatile compounds, dissociation of large-molecular-size oligomeric compounds (Bateman et al., 2011), formation of large-molecular-size compounds via oligomerization (Walhout et al., 2019), among others. To investigate the prevalence of these processes, Figure 6 shows the mass spectra colorcoded by the observed-change categories. For both OA types and all storage conditions, there are no clear trends that can be attributed to oligomerization or oligomer dissociation into monomers, as those would manifest as systematic molecular-size-dependent changes in the mass spectra (Bateman et al., 2011; Walhout et al., 2019), which is not evident in Figure 6. The only obvious change that can be gleaned from Figure 6 is the loss of some small-molecular-size species in conditions RC and RUC for pine-combustion OA, likely due to evaporation. For example, a major peak at 126.11 m/z with the molecular assignment C₆H₆O₃, likely maltol (an aromatic compound in pine needles), remains intact in condition F but is reduced significantly in conditions RC and RUC. Other observed changes are mostly associated with low-intensity peaks and most likely reflect a limitation of the technique rather than actual change. Therefore, in order to put the results in Figure 5 and Figure 6 in context, we tested the uncertainty in ESI-FTICR-MS analysis by reanalyzing the extracts of the pine-combustion OA sample (condition F) three months after extraction. We performed the analysis twice and compared the resulting mass spectra. As shown in SI Figure S2, the differences between the two mass spectra of this test sample reflect a similar extent of observed change as the stored samples compared to control. This indicates that the majority of the observed change in Figure 5 and Figure 6 is due to differences in instrument operation and not due to sample degradation.

OA chemical speciation results are often used to estimate bulk properties, such as the relative abundance of different elemental groups, average oxygen to carbon ratios (O/C), and average organic matter to organic carbon (OM/OC) ratios. As shown in Figure 7 and Table 1, there are no prominent difference in these properties among the different storage conditions and no clear advantage of covering the samples and/or storing them in a freezer.

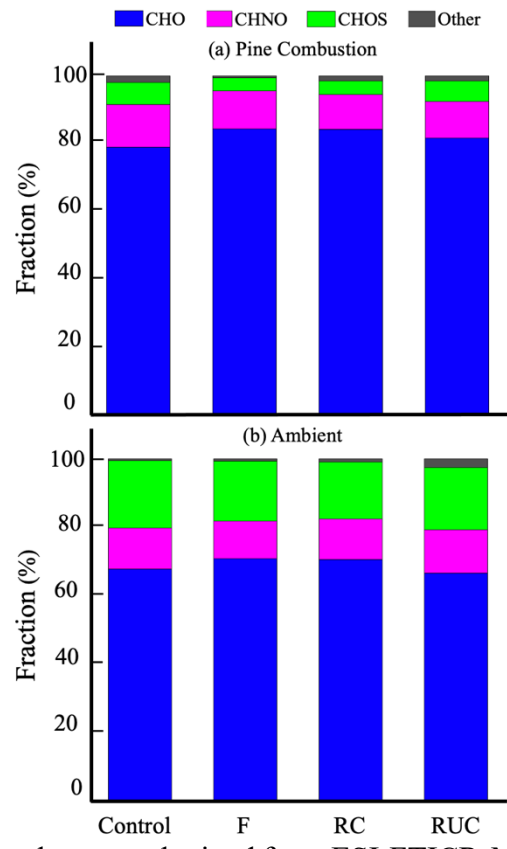


Figure 7. Fractions of elemental groups obtained from ESI-FTICR-MS measurements for (a) pine-combustion OA and (b) ambient OA for the different storage conditions.

Table 1. Average O/C and OM/OC of obtained from ESI-FTICR-MS measurements for (a) pine-combustion OA and (b) ambient OA for the different storage conditions.

| Sample | Storage Condition | Average O/C | Average OM/OC |
|-----------------|-------------------|-------------|---------------|
| Pine Combustion | Control | 0.31 | 1.55 |
| | F | 0.34 | 1.58 |
| Pine Combustion | RC | 0.32 | 1.56 |
| | RUC | 0.33 | 1.57 |
| | Control | 0.60 | 1.94 |
| Ambient | F | 0.56 | 1.89 |
| Ambient | RC | 0.54 | 1.86 |
| | RUC | 0.54 | 1.86 |

3.4. Effect of filter-storage conditions on retrieved imaginary part of the refractive indices

The imaginary part of the refractive indices (k) of the OA extracts retrieved from UV-vis absorption measurements for the different storage conditions are shown in Figure 8. To facilitate the discussion, the corresponding k at 550 nm (k_{550}) and wavelength dependence of k (w), obtained from power-law fits of the k versus λ data, are shown in Table 2. For toluene-combustion, all storage conditions led to a slight decrease in k_{500} and a corresponding increase in w relative to

control. However, these differences are likely due to limitations in the measurement techniques rather than actual differences in light-absorption properties. For pine-combustion, condition F had k values that are consistent with control. However, RC and RUC storage conditions led to an increase in k_{550} relative to control by approximately a factor of 1.5 and 2, respectively. The increase in k_{550} was associated with a decrease in w. This suggests that the observed change in light-absorption properties was driven by loss of species with relatively weak but highly wavelength-dependent absorption (small k_{550} and large w). These species are likely to have small molecular sizes (Saleh, 2020), which is consistent with the observed loss in small-molecular-size compounds for the RC and RUC conditions (Figure 6).

The RUC condition was chosen to investigate the effect of photobleaching on the retrieved k. As described above, no significant photobleaching was observed for either pine or toluene-combustion.

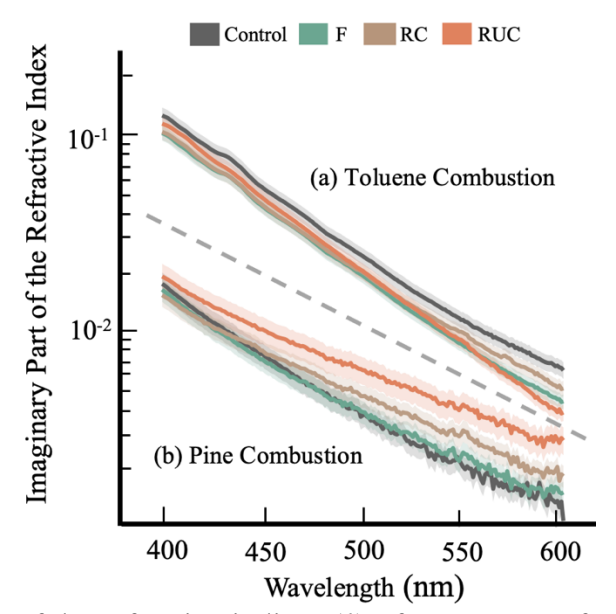


Figure 8. Imaginary part of the refractive indices (*k*) of OA extracts for toluene-combustion OA and pine-combustion OA for the different storage conditions. Shaded regions depict uncertainty bounds, calculated as shown in the SI.

Table 2. Imaginary part of the refractive indices at 550 nm (k_{550}) and the wavelength dependence of k toluene-combustion OA and pine-combustion OA for the different storage conditions.

| Sample | Storage Condition | k550 | w |
|-----------------------|-------------------|----------------------|------------------|
| | Control | 0.0114 ± 0.001 | 7.5 ± 0.005 |
| Toluene Combustion | F | 0.0085 ± 0.0007 | 7.65 ± 0.06 |
| Totuelle Collibustion | RC | 0.0098 ± 0.0009 | 7.57 ± 0.04 |
| | RUC | 0.0088 ± 0.0008 | 7.97 ± 0.055 |
| | Control | 0.002 ± 0.00028 | 6.82 ± 0.04 |
| Pine Combustion | F | 0.002 ± 0.00032 | 6.335 ± 0.06 |
| rine Combustion | RC | 0.0031 ± 0.0004 | 5.22 ± 0.035 |
| | RUC | 0.0042 ± 0.00067 | 4.85 ± 0.035 |

4. Conclusions

In this work, we show that the common practice of covering aerosol filter samples with aluminum foil and storing them in a freezer to avoid sample degradation does not provide any obvious advantage for OA chemical analysis using ESI-FTICR-MS. In thermal-optical analysis, however, storing in a freezer had a measurable effect in preserving the OC1 fraction, whereas some OC1 losses were observed for samples stored at room temperature. We note that we did not correct for positive artifacts in the thermal-optical analysis, and thus the loss in OC1 for the samples stored at room temperature was at least in part due to evaporation of adsorbed vapors. Therefore, it is possible that the advantage of storing in a freezer is overestimated. The only type of analysis where storing in a freezer was necessary to avoid significant artifacts was the retrieval of optical properties of pine-combustion OA from UV-vis measurements. Storing the samples at room temperature covered and uncovered led to an overestimation of k_{550} by a factor of 1.5 and 2, respectively. We attribute this artifact to evaporative loss of small-molecular-size species with relatively weak absorption. Exposing the samples to indoor laboratory lighting for a month (i.e. storing at RUC conditions) did not lead to any reduction in absorption that can be attributed to photobleaching.

Acknowledgments

Sampling of ambient aerosols was performed using the sampling port in Dr. Geoffrey Smith's laboratory. Optical analysis was preformed using the UV-Vis spectrometer in Dr. Amanda Frossard's laboratory. ESI- FTICR-MS measurements were performed at the University of Georgia Proteomics and Mass Spectrometry Core Facility.

Disclosure statement

The authors report there are no competing interests to declare.

414 Funding

This work was supported by the National Science Foundation, Division of Atmospheric and

416 Geospace Sciences under Grant AGS- 2144062

417 References

445

446

447

448

- 418 Apicella, B., Carpentieri, A., Alfè, M., Barbella, R., Tregrossi, A., Pucci, P., & Ciajolo, A.
- 419 (2007). Mass spectrometric analysis of large PAH in a fuel-rich ethylene flame.
- 420 *Proceedings of the Combustion Institute*, 31(1), 547–553.
- 421 https://doi.org/https://doi.org/10.1016/j.proci.2006.08.014
- Atwi, K., Cheng, Z., el Hajj, O., Perrie, C., & Saleh, R. (2022). A dominant contribution to light absorption by methanol-insoluble brown carbon produced in the combustion of biomass fuels typically consumed in wildland fires in the United States. *Environmental Science:*Atmospheres, 2(2), 182–191. https://doi.org/10.1039/D1EA00065A
- Atwi, K., Mondal, A., Pant, J., Cheng, Z., El Hajj, O., Ijeli, I., Handa, H., & Saleh, R. (2021).
 Physicochemical properties and cytotoxicity of brown carbon produced under different
 combustion conditions. *Atmospheric Environment*, 244, 117881.
 https://doi.org/https://doi.org/10.1016/j.atmosenv.2020.117881
- Atwi, K., Wilson, S. N., Mondal, A., Edenfield, R. C., Symosko Crow, K. M., el Hajj, O., Perrie,
 C., Glenn, C. K., Easley, C. A., Handa, H., & Saleh, R. (2022). Differential response of
 human lung epithelial cells to particulate matter in fresh and photochemically aged biomassburning smoke. *Atmospheric Environment*, 271, 118929.
 https://doi.org/https://doi.org/10.1016/j.atmosenv.2021.118929
- Badia, J. H., Ramírez, E., Bringué, R., Cunill, F., & Delgado, J. (2021). New Octane Booster
 Molecules for Modern Gasoline Composition. *Energy & Fuels*, 35(14), 10949–10997.
 https://doi.org/10.1021/acs.energyfuels.1c00912
- Bateman, A. P., Nizkorodov, S. A., Laskin, J., & Laskin, A. (2011). Photolytic processing of
 secondary organic aerosols dissolved in cloud droplets. *Physical Chemistry Chemical Physics*, 13(26), 12199–12212. https://doi.org/10.1039/C1CP20526A
- Bhattarai, H., Saikawa, E., Wan, X., Zhu, H., Ram, K., Gao, S., Kang, S., Zhang, Q., Zhang, Y.,
 Wu, G., Wang, X., Kawamura, K., Fu, P., & Cong, Z. (2019). Levoglucosan as a tracer of biomass burning: Recent progress and perspectives. *Atmospheric Research*, 220, 20–33.
 https://doi.org/https://doi.org/10.1016/j.atmosres.2019.01.004
 - Blair, S. L., MacMillan, A. C., Drozd, G. T., Goldstein, A. H., Chu, R. K., Paša-Tolić, L., Shaw, J. B., Tolić, N., Lin, P., Laskin, J., Laskin, A., & Nizkorodov, S. A. (2017). Molecular Characterization of Organosulfur Compounds in Biodiesel and Diesel Fuel Secondary Organic Aerosol. *Environmental Science & Technology*, 51(1), 119–127. https://doi.org/10.1021/acs.est.6b03304
- Browne, E. C., Zhang, X., Franklin, J. P., Ridley, K. J., Kirchstetter, T. W., Wilson, K. R., Cappa, C. D., & Kroll, J. H. (2019). Effect of heterogeneous oxidative aging on light absorption by biomass burning organic aerosol. *Aerosol Science and Technology*, *53*(6), 663–674. https://doi.org/10.1080/02786826.2019.1599321
- Chen, L.-W. A., Moosmüller, H., Arnott, W. P., Chow, J. C., Watson, J. G., Susott, R. A.,
 Babbitt, R. E., Wold, C. E., Lincoln, E. N., & Hao, W. M. (2007). Emissions from
 Laboratory Combustion of Wildland Fuels: Emission Factors and Source Profiles. *Environmental Science & Technology*, 41(12), 4317–4325.
 https://doi.org/10.1021/es062364i
- Chen, Y., & Bond, T. C. (2010). Light absorption by organic carbon from wood combustion.
 Atmospheric Chemistry and Physics, 10(4), 1773–1787. https://doi.org/10.5194/acp-10-1773-2010

- Cheng, Y., He, K. B., Duan, F. K., Zheng, M., Ma, Y. L., Tan, J. H., & Du, Z. Y. (2010).
 Improved measurement of carbonaceous aerosol: evaluation of the sampling artifacts and inter-comparison of the thermal-optical analysis methods. *Atmospheric Chemistry and Physics*, 10(17), 8533–8548.
- Cheng, Y., He, K., Du, Z., Engling, G., Liu, J., Ma, Y., Zheng, M., & Weber, R. J. (2016). The
 characteristics of brown carbon aerosol during winter in Beijing. *Atmospheric Environment*,
 127, 355–364. https://doi.org/https://doi.org/10.1016/j.atmosenv.2015.12.035
- Cheng, Z., Atwi, K., Hajj, O. el, Ijeli, I., Fischer, D. al, Smith, G., & Saleh, R. (2021).
 Discrepancies between brown carbon light-absorption properties retrieved from online and offline measurements. *Aerosol Science and Technology*, 55(1), 92–103.
 https://doi.org/10.1080/02786826.2020.1820940
- Cheng, Z., Atwi, K., Onyima, T., & Saleh, R. (2019). Investigating the dependence of light-absorption properties of combustion carbonaceous aerosols on combustion conditions.
 Aerosol Science and Technology, 53(4), 419–434.
 https://doi.org/10.1080/02786826.2019.1566593
- Chow, J. C., Wang, X., Sumlin, B. J., Gronstal, S. B., Chen, L.-W. A., Trimble, D. L., Kohl, S.
 D., Mayorga, S. R., Riggio, G., Hurbain, P. R., Johnson, M., Zimmermann, R., & Watson, J.
 G. (2015). Optical Calibration and Equivalence of a Multiwavelength Thermal/Optical
 Carbon Analyzer. *Aerosol and Air Quality Research*, 15(4), 1145–1159.
 https://doi.org/10.4209/aaqr.2015.02.0106
- Chow, J. C., Watson, J. G., Chen, L.-W. A., Chang, M. C. O., Robinson, N. F., Trimble, D., &
 Kohl, S. (2007). The IMPROVE_A Temperature Protocol for Thermal/Optical Carbon
 Analysis: Maintaining Consistency with a Long-Term Database. *Journal of the Air & Waste Management Association*, 57(9), 1014–1023. https://doi.org/10.3155/1047-3289.57.9.1014
- Chow, J. C., Watson, J. G., Robles, J., Wang, X., Chen, L.-W. A., Trimble, D. L., Kohl, S. D.,
 Tropp, R. J., & Fung, K. K. (2011). Quality assurance and quality control for
 thermal/optical analysis of aerosol samples for organic and elemental carbon. *Analytical and Bioanalytical Chemistry*, 401(10), 3141–3152. https://doi.org/10.1007/s00216-011-5103-3
- Dillner, A. M., Phuah, C. H., & Turner, J. R. (2009). Effects of post-sampling conditions on ambient carbon aerosol filter measurements. *Atmospheric Environment*, *43*(37), 5937–5943. https://doi.org/https://doi.org/10.1016/j.atmosenv.2009.08.009
 - el Hajj, O., Atwi, K., Cheng, Z., Koritzke, A. L., Christianson, M. G., Dewey, N. S., Rotavera, B., & Saleh, R. (2021). Two-stage aerosol formation in low-temperature combustion. *Fuel*, 304, 121322. https://doi.org/https://doi.org/10.1016/j.fuel.2021.121322
- EPA, U. S. (2009). US Environmental Protection Agency Air Quality System. Secondary US
 Environmental Protection Agency Air Quality System, 2009.
- Fioroni, G. M., Rahimi, M. J., Westbrook, C. K., Wagnon, S. W., Pitz, W. J., Kim, S., &
 McCormick, R. L. (2022). Chemical kinetic basis of synergistic blending for research
 octane number. *Fuel*, 307, 121865.
 https://doi.org/https://doi.org/10.1016/j.fuel.2021.121865

495

496

Goldstein, A. H., Koven, C. D., Heald, C. L., & Fung, I. Y. (2009). Biogenic carbon and
 anthropogenic pollutants combine to form a cooling haze over the southeastern United
 States. *Proceedings of the National Academy of Sciences*, 106(22), 8835–8840.
 https://doi.org/10.1073/pnas.0904128106

- Heald, C. L., Gouw, J. de, Goldstein, A. H., Guenther, A. B., Hayes, P. L., Hu, W., IsaacmanVanWertz, G., Jimenez, J. L., Keutsch, F. N., Koss, A. R., Misztal, P. K., Rappenglück, B.,
 Roberts, J. M., Stevens, P. S., Washenfelder, R. A., Warneke, C., & Young, C. J. (2020).
 Contrasting Reactive Organic Carbon Observations in the Southeast United States (SOAS)
 and Southern California (CalNex). *Environmental Science & Technology*, 54(23), 14923–14935. https://doi.org/10.1021/acs.est.0c05027
- Hettiyadura, A. P. S., Al-Naiema, I. M., Hughes, D. D., Fang, T., & Stone, E. A. (2019).
 Organosulfates in Atlanta, Georgia: anthropogenic influences on biogenic secondary
 organic aerosol formation. *Atmospheric Chemistry and Physics*, 19(5), 3191–3206.
 https://doi.org/10.5194/acp-19-3191-2019
- Ijaz, A., Kew, W., China, S., Schum, S. K., & Mazzoleni, L. R. (2022). Molecular
 Characterization of Organophosphorus Compounds in Wildfire Smoke Using 21-T Fourier
 Transform-Ion Cyclotron Resonance Mass Spectrometry. *Analytical Chemistry*, 94(42),
 14537–14545. https://doi.org/10.1021/acs.analchem.2c00916
- Islam, M. M., Neyestani, S. E., Saleh, R., & Grieshop, A. P. (2022). Quantifying brown carbon
 light absorption in real-world biofuel combustion emissions. *Aerosol Science and Technology*, 56(6), 502–516. https://doi.org/10.1080/02786826.2022.2051425
- Javed, T., Lee, C., AlAbbad, M., Djebbi, K., Beshir, M., Badra, J., Curran, H., & Farooq, A.
 (2016). Ignition studies of n-heptane/iso-octane/toluene blends. *Combustion and Flame*,
 171, 223–233. https://doi.org/10.1016/j.combustflame.2016.06.008
- Johnston, M. V, & Kerecman, D. E. (2019). Molecular Characterization of Atmospheric Organic
 Aerosol by Mass Spectrometry. *Annual Review of Analytical Chemistry*, 12(1), 247–274.
 https://doi.org/10.1146/annurev-anchem-061516-045135
- Kristensen, K., & Glasius, M. (2011). Organosulfates and oxidation products from biogenic hydrocarbons in fine aerosols from a forest in North West Europe during spring.
 Atmospheric Environment, 45(27), 4546–4556.
 https://doi.org/https://doi.org/10.1016/j.atmosenv.2011.05.063
- Kuwayama, T., Collier, S., Forestieri, S., Brady, J. M., Bertram, T. H., Cappa, C. D., Zhang, Q.,
 & Kleeman, M. J. (2015). Volatility of Primary Organic Aerosol Emitted from Light Duty
 Gasoline Vehicles. *Environmental Science & Technology*, 49(3), 1569–1577.
 https://doi.org/10.1021/es504009w
- Laskin, A., Laskin, J., & Nizkorodov, S. A. (2015). Chemistry of Atmospheric Brown Carbon.
 Chemical Reviews, 115(10), 4335–4382. https://doi.org/10.1021/cr5006167
- Laskin, A., Smith, J. S., & Laskin, J. (2009). Molecular Characterization of Nitrogen-Containing
 Organic Compounds in Biomass Burning Aerosols Using High-Resolution Mass
 Spectrometry. *Environmental Science & Technology*, 43(10), 3764–3771.
 https://doi.org/10.1021/es803456n
- Lee, S., Baumann, K., Schauer, J. J., Sheesley, R. J., Naeher, L. P., Meinardi, S., Blake, D. R.,
 Edgerton, E. S., Russell, A. G., & Clements, M. (2005a). Gaseous and Particulate Emissions
 from Prescribed Burning in Georgia. *Environmental Science & Technology*, 39(23), 9049–9056. https://doi.org/10.1021/es0515831
- Lee, S., Baumann, K., Schauer, J. J., Sheesley, R. J., Naeher, L. P., Meinardi, S., Blake, D. R.,
 Edgerton, E. S., Russell, A. G., & Clements, M. (2005b). Gaseous and Particulate
 Emissions from Prescribed Burning in Georgia. *Environmental Science & Technology*,

39(23), 9049–9056. https://doi.org/10.1021/es0515831

- 552 Lin, P., Aiona, P. K., Li, Y., Shiraiwa, M., Laskin, J., Nizkorodov, S. A., & Laskin, A. (2016).
- Molecular Characterization of Brown Carbon in Biomass Burning Aerosol Particles.
- *Environmental Science & Technology*, 50(21), 11815–11824.
- 555 https://doi.org/10.1021/acs.est.6b03024
- Lin, P., Bluvshtein, N., Rudich, Y., Nizkorodov, S. A., Laskin, J., & Laskin, A. (2017).
- Molecular Chemistry of Atmospheric Brown Carbon Inferred from a Nationwide Biomass Burning Event. *Environmental Science & Technology*, 51(20), 11561–11570.
- 559 https://doi.org/10.1021/acs.est.7b02276

565

- Lin, P., Fleming, L. T., Nizkorodov, S. A., Laskin, J., & Laskin, A. (2018). Comprehensive
 Molecular Characterization of Atmospheric Brown Carbon by High Resolution Mass
 Spectrometry with Electrospray and Atmospheric Pressure Photoionization. *Analytical Chemistry*, 90(21), 12493–12502. https://doi.org/10.1021/acs.analchem.8b02177
 - Mahilang, M., Deb, M. K., & Pervez, S. (2021). Biogenic secondary organic aerosols: A review on formation mechanism, analytical challenges and environmental impacts. *Chemosphere*, 262, 127771. https://doi.org/https://doi.org/10.1016/j.chemosphere.2020.127771
- Massabò, D., Caponi, L., Bove, M. C., & Prati, P. (2016). Brown carbon and thermal—optical
 analysis: A correction based on optical multi-wavelength apportionment of atmospheric
 aerosols. *Atmospheric Environment*, *125*, 119–125.
 https://doi.org/https://doi.org/10.1016/j.atmosenv.2015.11.011
- McMeeking, G. R., Kreidenweis, S. M., Baker, S., Carrico, C. M., Chow, J. C., Collett Jr., J. L.,
 Hao, W. M., Holden, A. S., Kirchstetter, T. W., Malm, W. C., Moosmüller, H., Sullivan, A.
 P., & Wold, C. E. (2009). Emissions of trace gases and aerosols during the open combustion
 of biomass in the laboratory. *Journal of Geophysical Research: Atmospheres*, 114(D19).
 https://doi.org/https://doi.org/10.1029/2009JD011836
- Michela, A., Barbara, A., Antonio, T., & Anna, C. (2008). Identification of large polycyclic
 aromatic hydrocarbons in carbon particulates formed in a fuel-rich premixed ethylene
 flame. *Carbon*, 46(15), 2059–2066.
 https://doi.org/https://doi.org/10.1016/j.carbon.2008.08.019
- Neyestani, S. E., Walters, S., Pfister, G., Kooperman, G. J., & Saleh, R. (2020). Direct Radiative
 Effect and Public Health Implications of Aerosol Emissions Associated with Shifting to
 Gasoline Direct Injection (GDI) Technologies in Light-Duty Vehicles in the United States.

 Environmental Science & Technology, 54(2), 687–696.
 https://doi.org/10.1021/acs.est.9b04115
- Nizkorodov, S. A., Laskin, J., & Laskin, A. (2011). Molecular chemistry of organic aerosols through the application of high resolution mass spectrometry. *Physical Chemistry Chemical Physics*, 13(9), 3612–3629.
- Perrino, C., Tofful, L., Torre, S. D., Sargolini, T., & Canepari, S. (2019). Biomass burning contribution to PM10 concentration in Rome (Italy): Seasonal, daily and two-hourly variations. *Chemosphere*, 222, 839–848.
- https://doi.org/https://doi.org/10.1016/j.chemosphere.2019.02.019
- Qi, Y., Fu, P., & Volmer, D. A. (2022). Analysis of natural organic matter via fourier transform
 ion cyclotron resonance mass spectrometry: an overview of recent non-petroleum
- applications. Mass Spectrometry Reviews, 41(5), 647–661.
- 595 https://doi.org/https://doi.org/10.1002/mas.21634

- Reid, J. S., Koppman, R., Eck, T. F., & Eleuterio, D. P. (2005). A review of biomass burning
 emissions part II: intensive physical properties of biomass burning particles, Atmos. Phys.
 Chem., 5, 799–825.
- Riva, M., Heikkinen, L., Bell, D. M., Peräkylä, O., Zha, Q., Schallhart, S., Rissanen, M. P., Imre,
 D., Petäjä, T., Thornton, J. A., Zelenyuk, A., & Ehn, M. (2019). Chemical transformations
 in monoterpene-derived organic aerosol enhanced by inorganic composition. *Npj Climate and Atmospheric Science*, 2(1), 2. https://doi.org/10.1038/s41612-018-0058-0
- Romonosky, D. E., Li, Y., Shiraiwa, M., Laskin, A., Laskin, J., & Nizkorodov, S. A. (2017).
 Aqueous Photochemistry of Secondary Organic Aerosol of α-Pinene and α-Humulene
 Oxidized with Ozone, Hydroxyl Radical, and Nitrate Radical. *The Journal of Physical Chemistry A*, 121(6), 1298–1309. https://doi.org/10.1021/acs.jpca.6b10900
- Russo, C., Alfè, M., Rouzaud, J.-N., Stanzione, F., Tregrossi, A., & Ciajolo, A. (2013). Probing structures of soot formed in premixed flames of methane, ethylene and benzene.
 Proceedings of the Combustion Institute, 34(1), 1885–1892.
 https://doi.org/https://doi.org/10.1016/j.proci.2012.06.127
- Saleh, R. (2020). From Measurements to Models: Toward Accurate Representation of Brown
 Carbon in Climate Calculations. *Current Pollution Reports*, 6(2), 90–104.
 https://doi.org/10.1007/s40726-020-00139-3
- Saleh, R., Cheng, Z., & Atwi, K. (2018). The Brown–Black Continuum of Light-Absorbing
 Combustion Aerosols. *Environmental Science & Technology Letters*, 5(8), 508–513.
 https://doi.org/10.1021/acs.estlett.8b00305
- Schneider, E., Czech, H., Popovicheva, O., Lütdke, H., Schnelle-Kreis, J., Khodzher, T., Rüger,
 C. P., & Zimmermann, R. (2022). Molecular Characterization of Water-Soluble Aerosol
 Particle Extracts by Ultrahigh-Resolution Mass Spectrometry: Observation of Industrial
 Emissions and an Atmospherically Aged Wildfire Plume at Lake Baikal. ACS Earth and
 Space Chemistry, 6(4), 1095–1107. https://doi.org/10.1021/acsearthspacechem.2c00017
- Schum, S. K., Brown, L. E., & Mazzoleni, L. R. (2020). MFAssignR: Molecular formula
 assignment software for ultrahigh resolution mass spectrometry analysis of environmental
 complex mixtures. *Environmental Research*, *191*, 110114.
 https://doi.org/https://doi.org/10.1016/j.envres.2020.110114
- Shao, C., Wang, H., Atef, N., Wang, Z., Chen, B., Almalki, M., Zhang, Y., Cao, C., Yang, J., &
 Sarathy, S. M. (2019). Polycyclic aromatic hydrocarbons in pyrolysis of gasoline surrogates
 (n-heptane/iso-octane/toluene). *Proceedings of the Combustion Institute*, 37(1), 993–1001.
 https://doi.org/https://doi.org/10.1016/j.proci.2018.06.087
- Simoneit, B. R. T. (2002). Biomass burning a review of organic tracers for smoke from incomplete combustion. *Applied Geochemistry*, 17(3), 129–162.
 https://doi.org/https://doi.org/10.1016/S0883-2927(01)00061-0
- Smith, J. S., Laskin, A., & Laskin, J. (2009). Molecular Characterization of Biomass Burning
 Aerosols Using High-Resolution Mass Spectrometry. *Analytical Chemistry*, 81(4), 1512–
 1521. https://doi.org/10.1021/ac8020664
- Stubbs, D. C., Humphreys, L. H., Goldman, A., Childtree, A. M., Kush, J. S., & Scarborough, D.
 E. (2021). An experimental investigation into the wildland fire burning characteristics of loblolly pine needles. *Fire Safety Journal*, *126*, 103471.
- https://doi.org/https://doi.org/10.1016/j.firesaf.2021.103471

Susaeta, A., & Gong, P. (2019). Economic viability of longleaf pine management in the
 Southeastern United States. Forest Policy and Economics, 100, 14–23.
 https://doi.org/https://doi.org/10.1016/j.forpol.2018.11.004

- Turpin, B. J., Huntzicker, J. J., & Hering, S. v. (1994). Investigation of organic aerosol sampling artifacts in the Los Angeles Basin. *Atmospheric Environment*, 28(19), 3061–3071.
- Turpin, B. J., Saxena, P., & Andrews, E. (2000). Measuring and simulating particulate organics in the atmosphere: problems and prospects. *Atmospheric Environment*, *34*(18), 2983–3013.
- Verma, V., Rico-Martinez, R., Kotra, N., King, L., Liu, J., Snell, T. W., & Weber, R. J. (2012).
 Contribution of Water-Soluble and Insoluble Components and Their
 Hydrophobic/Hydrophilic Subfractions to the Reactive Oxygen Species-Generating
 Potential of Fine Ambient Aerosols. *Environmental Science & Technology*, 46(20), 11384–11392. https://doi.org/10.1021/es302484r
 - Walhout, E. Q., Yu, H., Thrasher, C., Shusterman, J. M., & O'Brien, R. E. (2019). Effects of Photolysis on the Chemical and Optical Properties of Secondary Organic Material Over Extended Time Scales. *ACS Earth and Space Chemistry*, *3*(7), 1226–1236. https://doi.org/10.1021/acsearthspacechem.9b00109
 - Wang, Y., Hu, M., Lin, P., Tan, T., Li, M., Xu, N., Zheng, J., Du, Z., Qin, Y., Wu, Y., Lu, S., Song, Y., Wu, Z., Guo, S., Zeng, L., Huang, X., & He, L. (2019). Enhancement in Particulate Organic Nitrogen and Light Absorption of Humic-Like Substances over Tibetan Plateau Due to Long-Range Transported Biomass Burning Emissions. *Environmental Science & Technology*, 53(24), 14222–14232. https://doi.org/10.1021/acs.est.9b06152
 - Wong, J. P. S., Nenes, A., & Weber, R. J. (2017). Changes in Light Absorptivity of Molecular Weight Separated Brown Carbon Due to Photolytic Aging. *Environmental Science & Technology*, 51(15), 8414–8421. https://doi.org/10.1021/acs.est.7b01739
 - Wu, C., Huang, X. H. H., Ng, W. M., Griffith, S. M., & Yu, J. Z. (2016). Inter-comparison of NIOSH and IMPROVE protocols for OC and EC determination: implications for interprotocol data conversion. *Atmospheric Measurement Techniques*, *9*(9), 4547–4560. https://doi.org/10.5194/amt-9-4547-2016
 - Yang, L. H., Takeuchi, M., Chen, Y., & Ng, N. L. (2021). Characterization of thermal decomposition of oxygenated organic compounds in FIGAERO-CIMS. *Aerosol Science and Technology*, 55(12), 1321–1342. https://doi.org/10.1080/02786826.2021.1945529
- Zhang, H., Yee, L. D., Lee, B. H., Curtis, M. P., Worton, D. R., Isaacman-VanWertz, G.,
 Offenberg, J. H., Lewandowski, M., Kleindienst, T. E., Beaver, M. R., Holder, A. L.,
 Lonneman, W. A., Docherty, K. S., Jaoui, M., Pye, H. O. T., Hu, W., Day, D. A.,
 Campuzano-Jost, P., Jimenez, J. L., ... Goldstein, A. H. (2018). Monoterpenes are the
 largest source of summertime organic aerosol in the southeastern United States. *Proceedings of the National Academy of Sciences*, 115(9), 2038–2043.
 https://doi.org/10.1073/pnas.1717513115
- Zhang, X., Lin, Y.-H., Surratt, J. D., & Weber, R. J. (2013). Sources, Composition and
 Absorption Ångström Exponent of Light-absorbing Organic Components in Aerosol
 Extracts from the Los Angeles Basin. *Environmental Science & Technology*, 47(8), 3685–3693. https://doi.org/10.1021/es305047b